The evaluation value of ^{18}F-AV-133 PET/CT imaging in the Parkinson's disease crab-eating monkey model

Shilai Zhang[1] MD,
Yu Luo[1] Bs,
Zhi Yang[1] PhD,
Zhengzhong He[1] MD,
Ning Li[1] MD,
Hong Yang[1] MD,
Weiwei Pu[1] MD,
Ziya Liu[1] MD,
Taiyun Zhao[2] PhD,
Rongping Tang[3] BS,
Guoyuo Xiao[1] BS,
Hua Chai[1] MD

Shilai Zhang and Yu Luo contributed equally to this work and should be considered co-first author

1. Nuclear Medicine and Radiology, Guangxi Medical University Cancer Hospital,
2. Guangxi Key Laboratory of Bioactive Molecules Research and Evaluation,
3. Wincon TheraCells Biotechnologies Co., Ltd. in Nanning

Keywords: Parkinson's disease - Crab-eating monkey model - ^{18}F-AV-133 PET/CT

Corresponding author:
Guoyuo Xiao BS,
Nuclear Medicine and Radiology, Guangxi Medical University Cancer Hospital
xgy725@aliyun.com;

Hua Chai MD,
Nuclear Medicine and Radiology, Guangxi Medical University Cancer Hospital
404543738@qq.com

Received:
4 September 2024
Accepted revised:
9 November 2024

Abstract

Objective: To investigate the diagnostic value of fluorine-18-9-fluoropropyl-(+)-dihydrotetrabenazine (^{18}F-AV-133) positron emission tomography/computed tomography (PET/CT) for Parkinson's disease (PD) and the metabolic parameter changes in the PD macaque model. **Subjects and Methods:** Sixty three macaques were divided into an experimental group (n=55) and a normal group (n=8) for ^{18}F-AV-133 PET/CT imaging. In the experimental group, the macaques were injected with 1-methyl-4-phenyl-1,2,3,6-tetrahydropyridine (MPTP) solution into one side of the neck artery 2-3 months before imaging to induce unilateral striatal damage for self-control, while the normal group received no special treatment. After imaging, two nuclear medicine doctors conducted image analysis to determine the damaged side using visual inspection and compared the data with the actual damaged side to evaluate the model construction. The standardized uptake value (SUV) semi-quantitative analysis method was used to process the images, obtaining metabolic information of the damaged and preserved sides of the striatum, thalamus, occipital lobe, frontal lobe, parietal lobe, temporal lobe, and cerebellum in different sides of the normal group. Data analysis was performed using SPSS 25 to compare metabolic differences between different sides and evaluate the impact of modeling on the metabolism of other regions of the brain, with a significance level set at $P<0.05$. **Results:** Fluorine-18-AV-133 PET/CT imaging showed that the normal group of macaques exhibited relatively symmetrical radiotracer uptake in the bilateral striatal regions; the experimental group of PD macaque models showed completely asymmetrical radiotracer uptake in the left and right striatal regions, with model construction success rate of 100%. Semi-quantitative analysis using SUV revealed that the metabolic parameters SUVmax, SUVmean, metabolic tumor volume (MTV), and total lesion glycolysis (TLG) in the damaged striatal region of the experimental group of PD macaques were lower than those in the preserved side, with statistically significant differences ($t/z=8.277, 12.032, 8.827, 8.744$, $P<0.001$). The SUVmean in the damaged thalamus of the PD macaques was lower than in the preserved side (1.327 ± 0.354 vs. 1.490 ± 0.374), with a statistically significant difference ($t=2.352$, $P=0.02$).The metabolic parameters SUVmax, SUVmean, MTV, and TLG in the striatum of the normal group were higher than those in the preserved striatum of the experimental group, with $P<0.05$. **Conclusion:** Fluorine-18-AV-133 PET/CT can accurately assess the construction of PD macaque models and visualize the differences in metabolic parameters between different sides, making it useful for detecting monoaminergic terminal reduction in PD patients and providing a theoretical basis for the diagnosis and follow-up treatment of PD.

Hell J Nucl Med 2024; 27(3): 222-228 *Epub ahead of print: 14 December 2024* *Published online: 30 December 2024*

Introduction

Parkinson's disease (PD) is the second most prevalent neurodegenerative disorder, with a global prevalence exceeding six million individuals. Over the past three decades, the incidence of PD has increased by 2.5 times, making it a significant contributor to neurological dysfunction [1]. Despite substantial advancements in our understanding of its pathogenesis and epidemiology, the etiology of PD remains elusive, and no cure or preventive treatment has been discovered. Clinical symptoms and signs are the primary means for detecting and diagnosing PD; however, early diagnosis is challenging due to symptom overlap with other neurodegenerative diseases and the inability of imaging tests or biomarkers to provide accurate early diagnoses [2]. Positron emission tomography/computed tomography (PET/CT) is predominantly utilized in oncological diagnostics and therapy; nonetheless, it plays a crucial role in the diagnosis, monitoring of treatment response, and drug development for neurological disorders [3]. Molecular imaging with PET/CT and single photon emission computed tomography (SPECT) highlights neurotransmitter, metabolic, and inflammatory dysfunctions, which may distinguish disease phenotypes and have the potential to optimize precision medi-

cine in PD [4]. Radiotracers for evaluating dopaminergic function in the substantia nigra striatum in vivo can be classified into two categories: dopamine transporters (DAT) and type 2 vesicular monoamine transporters (VMAT2). Dopamine transporter, primarily located in dopamine axons and dendrites, plays a critical role in regulating extracellular dopamine concentrations [4]. Various DAT-targeted PET and SPECT radiotracers have been employed to identify and differentiate various neurodegenerative Parkinsonian syndromes and detect preclinical PD [5]. Type 2 vesicular monoamine transporter is responsible for packaging monoamine neurotransmitters into synaptic vesicles. As over 95% of VMAT2 in the striatum is associated with dopaminergic nerve terminals, VMAT2 in the striatum is considered a suitable biomarker for assessing dopaminergic innervation [6]. Fluorine-18-9-fluoropropyl-(+)-dihydrotetrabenazine (^{18}F-AV-133), a novel PET radiotracer targeting VMAT2 with a half-life of 109 minutes, effectively detects the reduction of monoaminergic terminals in PD patients [7]. Several studies have employed multi-tracer PET imaging methods, including DAT and VMAT2 radiotracers, in 1-methyl- 4-phenyl-1, 2, 3, 6-tetrahydropyridine (MPTP)-induced PD animal models to investigate early changes at dopaminergic synapses [8], age effects in MPTP-induced dopamine depletion [9], and assess neuronal loss in the substantia nigra striatum of MPTP-treated monkeys [10]. However, the extent of change or regulation of these presynaptic biomarkers and their correlation with disease progression warrant further exploration. This study aims to utilize the crab-eating monkey as the research animal, inducing a PD model through exposure to the neurotoxin MPTP. By acquiring ^{18}F-AV-133 PET/CT images via PET/CT scans, we will evaluate the modeling status and analyze the imaging characteristics of ^{18}F-AV-133 PET/CT imaging.

Subjects and Methods

Establishment of the Parkinson's monkey model

Provided by the Primate Laboratory of Lingkang Sainuo Biotechnology Co., Ltd. in Nanning, Guangxi (hereafter referred to as the Lingkang Laboratory) and the Guangxi Key Laboratory for Research and Evaluation of Bioactive Molecules, 63 crab-eating macaques were utilized as experimental animals. The control group comprised of 8 animals, while the experimental group consisted of 55 animals. Their ages were 13.13±4.190 years and 13.80±3.088 years respectively, with corresponding weights of 7.512±2.027kg and 5.969± 1.797 kg. All animals had undergone routine microbiological quarantine screening for viruses, bacteria, tuberculosis, and parasites, and were confirmed to be free from physical impairments. A summary of the fundamental clinical information of the experimental animals is presented in Table 1.

Animal husbandry, MPTP administration, post-modeling care, and behavioral analyses were conducted in the Lingkang Laboratory and the Guangxi Key Laboratory for Research and Evaluation of Bioactive Molecules. Each animal in the experimental group had to exhibit stable PD motor symptoms for at least one month before being classified as part of the experimental cohort. The laboratory is accredited by the Association for Assessment and Accreditation of Laboratory Animal Care (AAALAC) International, ensuring compliance with national standards for animal housing and guaranteeing optimal animal welfare during experimentation. The animal protocol for this study was reviewed and approved by the Institutional Animal Care and Use Committee (IACUC), emphasizing ethical considerations in animal research.

Table 1. *Basic clinical information of the crab-eating macaque.*

Clinical characteristics	Normal group (n=8)	Experimental group (n=55)
Sex		
Male	5 (62.50%)	29 (52.72%)
	3 (37.50%)	26 (47.28%)
Age (years)	13.13±4.190	13.80±3.088
Weight (kg)	7.512±2.027	5.969±1.797

Preparation and quality control of ^{18}F-AV-133

The production of ^{18}F using the Sumitomo HM-10HC cyclotron accelerator and its collection in the CFN200 multifunctional synthesis module for positron emission tomography drugs. After the collection of the target water, ^{18}F is captured using a QMA column. Following the capture, the synthesis of ^{18}F-AV-133 begins. (1) Elution and dehydration of ^{18}F. The ^{18}F adsorbed on the QMA column is rinsed into a reaction vial using a 0.9mL solution of K2.2.2/$K2CO_3$, and the reaction vial is heated to 100°C for drying and dehydration. After the vial is slightly dried, 0.3mL of anhydrous acetonitrile is added to the reaction vial for further drying and dehydration, using a two-step drying method to heat and evaporate the reaction vial. (2) Fluorination of ^{18}F-AV-133 precursor: After cooling for 60 seconds, the precursor dissolved in 1.0mg in 1.0mL of DMSO is added to the reaction vial. The reaction temperature is 100°C, and the reaction time is 10 minutes. (3) OasisHLB column solid-phase extraction purification: The reaction mixture in tube 1 is cooled for 100 seconds (≤60°C), then diluted with 3mL of deionized water and loaded into an OasisHLB 3mL drug cartridge. The cartridge is washed with 3mL of deionized water to remove any unreacted [^{18}F] fluoride. After drying the cartridge under a nitrogen flow, the final product is eluted with 1.0mL of ethanol, filtered through a 0.22μm membrane, and collected in a product collection vial for injection. The synthesis efficiency of ^{18}F-AV-133 is >25%, and the radiochemical purity is >95%.

Acquisition and processing of PET/CT images

This study utilized the American GE company's Discovery 710 PET/CT for image acquisition. Experimental animals were fasted for more than 6 hours before anesthesia. Prior to PET/CT imaging, intramuscular injection anesthesia was administered with 7-10mg/kg of ketamine hydrochloride and 0.1mL/kg of diazepam injection solution, with a concentration of

5mg/mL. The ^{18}F-AV-133 imaging agent was injected 30 minutes before the experimental animal PET/CT scan. Using the OM line as a positioning reference, with the OM line perpendicular to the ground as the standard, the head position of the experimental animals was fixed. After confirming that the head position met the standard, a specialized organic glass head holder was used with a 5-point fixation method, with fixation points at both ears (2 points) and the skull (1 point). The parameters for the 64-slice CT scan were: tube voltage 120kV, tube current 110mAs; rotation time 0.5s, slice thickness 1.25mm, pitch 0.8mm, matrix 512×512. Positron emission tomography images were acquired in 3D scans, with a duration of 2min/bed, and 7-8 beds per case. For blurry or poor quality images, a re-scan should be arranged. After image acquisition, CT attenuation correction was applied, and the images were reconstructed using the ordered subset expectation maximization method. The CT and PET images were fused using image fusion software to obtain maximal intensity projection images (MIP), cross-sectional images, coronal and sagittal views, individual CT images, individual PET images, and fused PET/CT images. After obtaining the PET/CT images, two nuclear medicine doctors above the attending physician level independently reviewed the images, and used post-processing MedEx software to read and analyze the images, identifying the maximum level of striatal imaging and outlining the region of interest (ROI) on the lesion side, as well as a similarly sized ROI on the preserved side for symmetry. The computer automatically measured the maximum standardized uptake value (SUVmax), SUVmean, MTV, and TLG values of the ROI. Region of interest of approximately 2cm were outlined in the bilateral thalamus, occipital lobe, frontal lobe, temporal lobe, parietal lobe, and cerebellum, to obtain the corresponding SUVmean values.

Statistical analysis

This study used SPSS 25.0 statistical software to analyze the data. All data were subjected to tests for normality and homogeneity of variance. Data that met the criteria for normal distribution were expressed as mean±standard deviation, and between-group comparisons were made using t-tests. Data that were skewed were expressed as median [M (P25, P75)], and between-group comparisons were made using the Mann-Whitney U test. A significance level of $P<0.05$ was considered statistically significant.

Results

Differential group feeding patterns in crab-eating macaques revealed by imaging results

Fluorine-18-AV-133PET/CT imaging showed a success rate of 100% in the bilateral striatum of the PD model in macaque monkeys. In the normal group, experimental animals exhibited relatively symmetric radioactive foci in the bilateral striatum area, forming a "figure-eight" imaging pattern (Figure 1A). The PD monkey model in the experimental group showed bright areas of radioactive accumulation on the healthy side, while the affected side exhibited sparse or absent radioactive distribution in dark areas (Figure 1B).

Comparative analysis of metabolic parameters in different body parts of the experimental crab-eating macaques

The semi-quantitative analysis results of SUV in the experimental group PD monkeys showed that the metabolic parameters SUVmax, SUVmean, MTV, and TLG of the damaged striatum were lower than the intact side, and the differences were statistically significant ($t/z=8.277, 12.032, 8.827, 8.744$, $P<0.001$). The results are shown in Table 2. The SUVmean of the damaged thalamus in the experimental group PD monkeys was lower than the intact side (1.327 ± 0.354 vs. 1.490 ± 0.374), and the difference was statistically significant ($t=2.352$, $P=0.02$). The SUVmean of the damaged occipital lobe, frontal lobe, temporal lobe, and cerebellum were lower than the intact side, with no statistically significant differences ($P>0.05$). The SUVmean of the damaged parietal lobe was higher than the intact side, with no statistically significant difference ($P>0.05$). The results are shown in Table 3.

Comparison of metabolic parameters in different parts of the body of normal crab-eating macaques

No significant differences were observed in metabolic para-

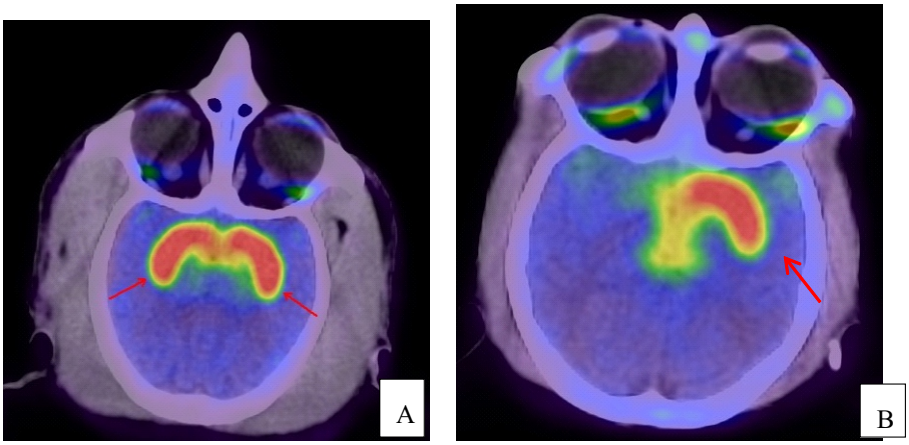

Figure 1. A shows the PET/CT findings of a normal crab-eating macaque, while B shows the PET/CT findings of a crab-eating macaque with striatal damage on the right side.

meters between the left and right striatum, parietal lobe, occipital lobe, frontal lobe, temporal lobe, and cerebellum in the control group of crab-eating macaques (all P>0.05), as shown in Tables 4 and 5.

Comparison of metabolic parameters of the normal group striatum and the experimental group reserved striatum

The metabolism parameters SUVmax, SUVmean, MTV, and TLG of the normal group in the bilateral striatum are all higher than those of the experimental group in the reserved striatum metabolism parameters, with all P values <0.05, as shown in Table 6.

Discussion

So far, the non-human primate PD model induced by MPTP is the animal model closest to the clinical characteristics of PD patients, and is the most ideal PD animal model under ideal conditions [10]. The PD monkey model constructed by it is very similar to primary PD in terms of pathological, physiolo-gical, neurotransmitter changes, and response to treatment. In terms of model evaluation, the more commonly used mo-lecular and functional imaging techniques are SPECT/CT, PET/CT, MRI, etc. In this study, ^{18}F-AV-133 PET/CT was used to evaluate the construction of the

Table 2. *Comparison of metabolic parameters of the bilateral striatum in the experimental group of rhesus monkeys.*

Features	Retention side	Damage side	Difference/Median difference and 95%CI	t/z	P
	Mean±SD/M(P25,P75)				
SUVmax	7.290 (5.960,8.610)	3.150(2.560,3.830)	4.020(3.400-4.680)	8.277	＜0.001
SUVmean	4.412±1.235	2.118±0.688	2.294(1.915-2.673)	12.032	＜0.001
MTV	259.510(213.150,289.420)	58.170(46.840,73.240)	191.060(172.980-209.320)	8.827	＜0.001
TLG	5.210(4.430,7.890)	0.550(.330,0.550)	4.670(4.290-5.280)	8.744	＜0.001

Table 3. *Comparison of metabolic parameters (SUVmean) in bilateral thalamus and cerebral lobes between the experimental group of crab-eating macaques.*

Side	Retention side	Damage side	Difference and 95%CI	t	P
	Mean±SD(SUVmean)				
Occipital lobe	1.218±0.374	1.181±0.375	0.036(0.104-0.178)	0.517	0.606
Thalamus	1.490±0.374	1.327±0.354	0.163(0.025-0.301)	2.352	0.020
Frontal lobe	1.528±0.427	1.438±0.384	0.090(0.063-0.243)	1.162	0.248
Parietal lobe	1.396±0.384	1.397±0.388	.003(0.145-0.146)	0.005	0.996
Temporal lobe	1.619±0.377	1.555±0.375	0.064(0.077-0.206)	0.897	0.372
Cerebellum	1.337±0.445	1.319±0.413	0.018(0.143-0.181)	0.228	0.820

Table 4. *Comparison of metabolic parameters of the striatum in the normal group of crab-eating macaques on the left and right sides.*

Features	Right side	Left side	Difference and 95%CI	t	P
	Mean±SD				
SUVmax	11.945±2.431	12.140±2.455	0.195(2.425-2.815)	0.160	0.875
SUVmean	7.050±1.384	7.150±1.448	0.100(1.419-1.619)	0.141	0.890
MTV	293.737±39.085	319.607±47.146	25.870(20.569-72.309)	1.195	0.253
TLG	9.576±2.139	9.030±1.872	0.546(1.609-2.702)	0.543	0.596

Table 5. *Comparison of metabolic parameters in the bilateral thalamus and brain lobes of normal macaques.*

Features	Right side	Left side	Difference and 95%CI	t	P
	Mean±SD(SUVmean)				
Occipital lobe	1.595±0.19559	1.598±0.22706	0.003(0.223-0.231)	0.035	0.972
Thalamus	2.015±0.153	1.987±0.218	0.027(0.174-0.229)	0.291	0.775
Frontal lobe	1.977±0.274	1.971±0.165	0.006(0.236-0.248)	0.055	0.957
Parietal lobe	1.766±0.251	1.766±0.291	0.000(0.292-0.292)	0.000	1.000
Temporal lobe	1.907±0.237	1.935±0.205	0.275(0.111-0.265)	0.248	0.808
Cerebellum	1.707±0.268	1.706±0.203	0.001(0.254-0.256)	0.010	0.992

Table 6. *Comparison of metabolic parameters between the normal group striatum and the experimental group reserved side striatum.*

Features	Normal group	Experimental group	Difference orreserved side striatum	Median difference(95%CI)	t/z	P
	Mean±SD/M(P25,P75)					
SUVmax						
Right	11.945±2.431		7.398±2.231	4.546(2.839-6.253)	5.327	<0.001
Left	12.140±2.455			4.741(3.032-6.450)	5.548	<0.001
SUVmean						
Right	7.050±1.384		4.412±1.235	2.637(1.689-3.586)	5.561	<0.001
Left	7.150±1.448			2.737(1.782-3.692)	5.734	<0.001
MTV						
Right	284.935(266.125,337.205)		259.510(213.150,289.420)	40.925(1.030-77.700)	1.879	0.041
Left	303.020(285.590,352.547)			64.840(18.010-107.590)	2.869	0.004
TLG						
Right	9.576±2.139		5.853±2.370	3.722(1.948-5.496)	4.196	<0.001
Left	9.030±1.872			3.176(1.422-4.930)	3.621	<0.001

vesicular monoamine transporter is responsible for packaging all monoamine neurotransmitters, so ^{18}F-AV-133-VMAT2 imaging not only targets dopaminergic nerve innervation, but can also spread to other monoaminergic neurons, inclu-ding serotonin and norepinephrine [11]. Therefore, ^{18}F-AV-133 images can provide quantification in the substantia nig-ra and midbrain, which may play an important role in Parkin-son's disease and other parkinsonian syndromes [12]. Since the motor dysfunction symptoms of PD progress from unila-teral to bilateral during the course of the disease, the asym-metry of striatal imaging is an important indicator for early detection of PD. The results of this study found that ^{18}F-AV-133 has good targeting specificity for the striatum, with the normal striatum in the PET/CT image showing a "figure-eig-ht" pattern of left-right basic symmetry, while the experi-mental group shows significantly lower radioactive uptake on the damaged side of the striatum compared to the preser-ved side, with complete asymmetry in the image, and higher contrast with the surrounding background. Therefore, the sensitivity and accuracy of diagnosing the damaged side of the PD macaque model are both 100%, showing several advantages in terms of high resolution, high sensitivity, and better targeting. This is similar to the results of Hsiao [13], who compared the diagnostic value of two tracers targeting DAT (^{99m}Tc-TRODAT-1) and VMAT2 (^{18}F-AV-133) for PD, and found that ^{18}F-AV-133 PET showed similar ability to differentiate between PD and normal control subjects as ^{99m}Tc-TRODAT-1 SPECT, with shorter imaging time and better image quality, as well as better stability in quantitative analysis, and higher correlation with clinical features of lateralized scoring. Therefore, ^{18}F-AV-133 imaging may be better used for early detection of PD in clinical applications.

This study demonstrates that the metabolic parameters SUVmax, SUVmean, MTV, and TLG in the lesioned striatum of the experimental PD monkey group were significantly lower than those in the preserved side, suggesting a marked decrease in uptake function in the striatum affected by MPTP- induced damage. This finding aligns with previous research on PD [13-16]. To investigate metabolic alterations in the preserved striatum of the experimental group, we compared the metabolic parameters of the bilateral striatum in the control group with those of the preserved side in the experimental group. The results revealed that the metabolic parameters of the preserved striatum in the experimental group were lower than in the control group, with statistically significant differences, implying that the preserved striatum is influenced by MPTP toxicity and/or the progression of PD, consistent with the asymmetric progression of the disease. The rate of decline in VMAT2, which reflects dopamine neuronal loss in PD, remains unclear. Prior research has reported distinct progression patterns for DAT and VMAT2 in PD animal models [17]. A recent study in non-human primate PD models showed that VMAT2 loss precedes DAT reduction during the asymptomatic phase [18]. However, more studies with asymptomatic or early-stage subjects and longitudinal designs are needed to thoroughly address this issue. Furthermore, we also compared metabolic parameter changes in the bilateral parietal, occipital, frontal, temporal lobes, thalamus, and cerebellar hemispheres. The mean SUV in the lesioned thalamus was found to be lower than in the preserved side with statistical significance; however, no difference was observed between thalami in the control group. Potential explanations include: (I) damage from MPTP toxicity; (II) the thalamus' proximity to the striatum, making it more susceptible to metabolic parameter changes; (III) the impact of PD progression on the metabolism and function of thalamic nuclei; and (IV) influences of image quality. Given the scarcity of related studies, further research with larger sample sizes is required for confirmation. Future investigations should also strive to enhance the spatial resolution of PET/CT scans to minimize the effects of adjacent tissue.

This study is a small sample study, and there are certain differences between animal models and human PD that occur naturally, lacking comparative studies with real humans. In addition, the subgroups of PD disease in this study are limited. Therefore, it is necessary to further verify with a larger sample size, a wider range of staged Parkinson's disease patients, and longitudinal studies.

In conclusion, ^{18}F-AV-133PET/CT can accurately assess the construction of PD crab-eating monkey models and visualize the differences between different side metabolic parameters, which can be used to detect the decrease of monoamine terminals in PD patients, providing theoretical basis for the diagnosis and treatment follow-up of PD.

The authors declare that they have no conflicts of interest.

Funding

This work was supported by the Youth Science Foundation of Guangxi Medical University (GXMUYSF202356), and the Scientific and Technological Innovation Major Base of Guangxi (No.2022-36-Z05/GXSWBX202203, No.2022-36-Z05/GXSWBX202204,No.2022-36-Z05/GXSWBX202205),the Guangxi University Young and middle-aged teachers' scientific research Ability Improvement Project (2023KY0084), the Health Commission of Guangxi Zhuang Autonomous Region (Z20210836).

Ethics declaration

The animal protocol for this study was reviewed and approved by the Institutional Animal Care and Use Committee (IACUC)(approval number:WD00164 and UPP-IACUC-2023-S0104AEly), emphasizing ethical considerations in animal research.

Acknowledgements

We thank to Guangxi Nanning spirit concept noble families primate laboratory biological technology co., LTD (hereinafter referred to as the spirit, laboratory) and Guangxi research and evaluation of key laboratory of bioactive molecules provide 63 cynomolgus monkeys. We thank the Guangxi Medical University Cancer Hospital for their support of this study.

Bibliography

1. Sasikumar S, Strafella A P. The challenging quest of neuroimaging: From clinical to molecular-based subtyping of Parkinson disease and atypical parkinsonisms. *Handb Clin Neurol* 2023; 192: 231-58.
2. Tolosa E, Garrido A, Scholz S W et al. Challenges in the diagnosis of

3. Roth KS, Voltin CA, van Heek L et al. Dual-Tracer PET/CT Protocol with ^{18}F-FDG and [^{68}Ga]Ga-FAPI-46 for Cancer Imaging: A Proof of Concept. *J Nucl Med* 2022; 63(11): 1683-6.
4. Beauchamp LC, Dore V, Villemagne VL et al. Using ^{18}F-AV-133 VMAT2 PET Imaging to Monitor Progressive Nigrostriatal Degeneration in Parkinson Disease. *Neurology* 2023; 101(22): e2314-e2324.
5. Lu C, Weng Y, Chen M et al. ^{99m}Tc-TRODAT-1 Imaging of Multiple System Atrophy. *J Nucl Med* 2004; 45(1): 49-55.
6. Martin W R, Wieler M, Stoessl A J et al. Dihydrotetrabenazine positron emission tomography imaging in early, untreated Parkinson's disease. *Ann Neurol* 2008; 63(3): 388-94.
7. Okamura N, Villemagne V L, Drago J et al. In Vivo Measurement of Vesicular Monoamine Transporter Type 2 Density in Parkinson Disease with ^{18}F-AV-133[J]. *J Nucl Med* 2010; 51(2): 223.
8. Chen M K, Kuwabara H, Zhou Y et al. VMAT2 and dopamine neuron loss in a primate model of Parkinson's disease. *J Neurochem* 2008; 105(1): 78-90.
9. Doudet D J, Rosa-Neto P, Munk O L et al. Effect of age on markers for monoaminergic neurons of normal and MPTP-lesioned rhesus monkeys: A multitracer PET study. *Neuroimage* 2006; 30(1): 26-35.
10. Tian L, Karimi M, Loftin S K et al. No differential regulation of dopamine transporter (DAT) and vesicular monoamine transporter 2 (VMAT2) binding in a primate model of Parkinson disease. *PLoS One* 2012; 7(2): e31439.
11. Zeng X S, Geng W S, Jia J J. Neurotoxin-Induced Animal Models of Parkinson Disease: Pathogenic Mechanism and Assessment. *ASN Neuro* 2018; 10: 1663354718.
12. Eiden L E, Schäfer M K, Weihe E et al. The vesicular amine transporter family (SLC18): amine/proton antiporters required for vesicular accumulation and regulated exocytotic secretion of monoamines and acetylcholine. *Pflügers Archiv* 2004; 447(5): 636-40.
13. Tirassa P, Schirinzi T, Raspa M et al. What substance P might tell us about the prognosis and mechanism of Parkinson's disease? *Neurosci Biobehav Rev* 2021; 131: 899-911.
14. Hsiao I T, Weng Y H, Lin W Y et al. Comparison of ^{99m}Tc-TRODAT-1 SPECT and ^{18}F-AV-133 PET imaging in healthy controls and Parkin-son's disease patients. *Nucl Med Biol* 2014; 41(4): 322-9.
15. Kerstens V S, Fazio P, Sundgren M et al. Longitudinal DAT changes measured with [^{18}F]FE-PE2I PET in patients with Parkinson's disease; a validation study. *Neuroimage Clin* 2023; 37: 103347.
16. Dai Y, Sa R, Guan F et al. A Purification Method of ^{18}F-FP-(+)-DTBZ via Solid-Phase Extraction With Combined Cartridges. *Front Med* 2021; 8: 693632.
17. Palumbo B, Fravolini M L, Nuvoli S et al. Comparison of two neural network classifiers in the differential diagnosis of essential tremor and Parkinson's disease by ^{123}I-FP-CIT brain SPECT. *Eur J Nucl Med Mol Imaging* 2010; 37(11): 2146-53.
18. Kilbourn M R, Kuszpit K, Sherman P. Rapid and differential losses of in vivo dopamine transporter (DAT) and vesicular monoamine transporter (VMAT2) radioligand binding in MPTP-treated mice. *Synapse* 2000; 35(4): 250-5.
19. Kim H Y, Lee J, Kim H J et al. PLCgamma1 in dopamine neurons critically regulates striatal dopamine release via VMAT2 and